JOURNAL OF CATALYSIS 96, 261–275 (1985)

The Reduction Behavior of Supported Iron Catalysts in Hydrogen or Carbon Monoxide Atmospheres

A. J. H. M. KOCK, H. M. FORTUIN, AND J. W. GEUS

Department of Inorganic Chemistry, State University of Utrecht, Croesestraat 77a, 3522 AD Utrecht, The Netherlands

Received November 9, 1984; revised April 12, 1985

The reduction behavior of iron catalysts supported on magnesia or alumina was investigated using *in situ* high-field magnetization measurements, thermomagnetic analysis, temperature-programmed reduction, and X-ray diffraction. The complete disappearance of ferro- or ferrimagnetic behavior preceding the reduction to α-Fe during the reduction by hydrogen of iron/magnesia catalysts provided evidence for the presence of a well-stabilized FeO phase at temperatures where bulk FeO is metastable. The concept that a temporary stabilization of an FeO phase during reduction is indicative of a considerable metal(oxide)–support interaction appeared to be useful in the characterization of iron/alumina catalysts. To determine the presence of an iron oxide species which has no marked interaction with the support, thermomagnetic analysis was performed during temperature-programmed reduction by hydrogen or carbon monoxide. During reduction with carbon monoxide the ferri- or ferromagnetism displayed by the iron/alumina catalysts investigated disappeared completely, while the formation of iron carbides preceding the reduction beyond FeO was not observed. Unsupported α-FeOOH or α-Fe_2O_3, on the other hand, reacted to θ-Fe_3C prior to the disappearance of the ferro- or ferrimagnetism.

INTRODUCTION

The reduction of unsupported iron oxides and that of various supported and/or promoted iron catalysts have been studied extensively (*1–5*). Especially, the kinetics of the reduction process has been the subject of a large number of papers (*6, 7*). The reaction proceeds in a stepwise manner:

$$\underset{\text{hematite}}{\alpha\text{-}Fe_2O_3} \rightarrow \underset{\text{magnetite}}{Fe_3O_4} \rightarrow \underset{\text{wustite}}{FeO} \rightarrow \underset{\text{iron}}{\alpha\text{-}Fe}$$

It should be noted that wustite is thermodynamically metastable with respect to magnetite and iron at temperatures below 843 K.

Assuming shrinking core behavior, Spitzer *et al.* (*8*) presented a very comprehensive description of the stepwise reduction of unsupported hematite. Both the intrinsic reduction kinetics and the pore diffusion contribute to the overall rate of reduction. Spherical pellets of unsupported hematite are assumed to reduce topochemically at three advancing interfaces: hematite/magnetite, magnetite/wustite, and wustite/iron. The gaseous reactant has to be transported from the bulk gas phase to the outer surface of the particle, followed by diffusion through the porous solid phase to the nearest interface. Chemical equilibrium is attained at the interface, and subsequently the remaining reductant diffuses to the next interface, and the cycle is repeated. Outward transport of the gaseous product follows the opposite pattern. It should be stressed that sharp interfaces between reacted and unreacted zones are only observed when the overall rate of reduction is limited by pore diffusion.

Although a generalized description of the reduction process incorporates a sequence of transport and chemical steps acting in series, many investigators consider the reduction process to be predominantly chemically controlled at the interface between reduced and unreduced zones (*9, 10*). At high temperatures the reduction of bulk he-

0021-9517/85 $3.00

matite appeared to be chemically controlled at the wustite/iron interface. In the temperature region where wustite is metastable with respect to disproportionation, the reduction process is considered to be controlled at the magnetite/iron interface (*7*). The shrinking core model turned out to describe satisfactorily the reduction of magnetite (promoted with K_2O, CaO, and Al_2O_3) by hydrogen, provided that carefully dried gas was passed over the catalyst. Small amounts of water, however, affected the rate of reduction considerably, causing the model to become invalid (*11, 12*). Pattek-Janczyk and Hrynkiewicz (*13*) performed Mössbauer spectroscopy as a complementary technique to thermogravimetry to analyze quantitatively the iron phases present during the reduction of the triply promoted magnetite mentioned above by hydrogen at 673 K. Both the amounts of magnetite and wustite initially present gradually decreased in favor of iron. As magnetite did not appear to reduce to an intermediate FeO phase prior to reduction to α-Fe, the assumption that the reduction proceeds at the magnetite/iron interface in the presence of small amounts of alumina (up to 3 wt% (*14*)) seems to be justified.

While the investigations mentioned above concern the reduction behavior of unsupported iron oxides or promoted magnetite, supported catalysts of low metal loading display a different behavior. Mössbauer experiments on a 0.05 wt% Fe/η-Al_2O_3 catalyst indicated that the reduction beyond Fe^{2+} did not proceed. Even after a severe reduction procedure (hydrogen treatment at 970 K during 8 ks) no metallic iron was observed (*15*). Also, iron oxide supported on SiO_2 (~3 wt% metal loading) was found not to reduce to metallic iron (*16*). Furthermore, Boudart *et al.* (*17*), investigating iron/magnesia catalysts with a metal loading varying from 1 up to 40 wt%, found evidence for the presence of an FeO phase forming a solid solution with the MgO support after reduction for 80 ks at 700 K both by Mössbauer spectroscopy and by an accurate determination of the cell parameters from X-ray diffraction patterns.

Depending on the nature of the support material chosen, part of the iron can thus not be reduced beyond Fe^{2+}. This can be associated with a metal(oxide)–support interaction or, more explicitly, with the formation of an interfacial compound between the metal(oxide) and support. Thus, it is conceivable that after the above reduction pretreatments catalysts of low metal loading do not contain metallic iron at all.

The present work was initiated to check the assumptions underlying the description of the kinetics of reduction of supported iron catalysts (iron/aluminum ratio = 0.5), viz. the presence of exclusively Fe_2O_3, Fe_3O_4, and/or α-Fe on supported catalysts at temperatures below 843 K. In this study our aim is to investigate the stabilization of transient bulk iron suboxides by the support during the reduction by hydrogen or carbon monoxide. Our working hypothesis, developed from the work on Fe/MgO catalysts, was that the presence of a metastable iron suboxide could be an indication of a strong metal(oxide)–support interaction. We performed experiments (i) to collect further evidence for the presence of wustite on a magnesia support and (ii) to investigate the sequence of the consecutive steps in the reduction of iron/alumina catalysts. The iron/magnesia catalysts containing 20 wt% Fe (referred to a dry reduced sample) were prepared by injection of a solution of iron nitrate into a suspension of magnesium hydroxycarbonate or magnesia. The iron/alumina catalysts were prepared by injection of a basic solution into a suspension of alumina in an acid solution of iron nitrate or by injection of a solution of iron nitrate into a suspension of alumina kept at a pH of 6.0. *In situ* high-field magnetization measurements, temperature-programmed reduction (TPR), and X-ray diffraction experiments were used in combination with thermomagnetic analysis to gain insight into the reduction mechanism.

A thorough understanding of the reduc-

tion process enables us to establish the status of a catalyst after the reduction pretreatment, which in turn greatly facilitates the interpretation of subsequent characterization measurements.

EXPERIMENTAL

Apparatus and procedures. Quantitative temperature-programmed reduction experiments were performed in a conventional atmospheric flow reactor (i.d. 8.0 mm). Hydrogen consumption was monitored by measurement of the thermal conductivity of the effluent gas. Product water was collected in a cold trap (acetone(s)/acetone(l)) localized between the reactor and the thermal conductivity detector. Hydrogen/argon mixture, obtained from Hoekloos bv, was deoxygenated over a copper catalyst (BASF R-3-11) and subsequently dehydrated over a column containing molecular sieve (Linde 4A). Typically, a quantity of catalyst containing 0.25 mmol of Fe was reduced in a 10 vol% hydrogen/argon mixture at a flow rate of 0.80 ml s^{-1} (heating rate 0.08 K s^{-1}).

Qualitative solid-phase analysis was carried out by X-ray diffraction (Debye–Scherrer), using Fe$K\alpha_{1,2}$ radiation. X-Ray patterns were measured using a microdensitometer (Jenoptik MD 100).

The magnetic susceptibility data were obtained via a modified Weiss-extraction technique, using an apparatus which has been described elsewhere (*18*). Samples containing 2.4 mmol of Fe could be magnetized at magnetic field strengths up to 0.52 MA m^{-1} (1 MA m^{-1} = 1.26 × 10^4 Oe), in a flow of reductant which was either 5 vol% carbon monoxide/helium or 10 vol% hydrogen/argon. *In situ* magnetization measurements could be performed in the temperature range 100–770 K. Optionally, a temperature program could be applied. In this investigation a heating/cooling rate of 0.08 K s^{-1} was chosen.

Thermomagnetic curves were measured at maximum magnetic field strength. The quartz sample-holder was connected via a leakage valve to a Pyrex high-vacuum system equipped with a quadrupole mass spectrometer (Leybold-Heraeus Q 200). High-purity carbon monoxide (N48) was supplied by AGA bv, and was used without further purification. Helium, purchased from Hoekloos bv, was passed over a column containing activated carbon at liquid-nitrogen temperature, and the 10 vol% hydrogen/argon mixture was consecutively deoxygenated over a Pd–Al_2O_3 catalyst and dehydrated over a column containing molecular sieve (Linde 4A).

N_2 BET surface areas were measured using a Carlo Erba Sorptomatic Series 1800.

Catalysts. Iron/magnesia catalyst, referred to as Fe-MHC, was prepared according to the procedure described by Boudart *et al.* (*17*). A slurry of 10 g magnesium hydroxycarbonate (MHC) in 150 ml demineralized water was heated to 340 K. Then 150 ml of a solution of $Fe(NO_3)_3 \cdot 9H_2O$ (Merck, p.a.) was added rapidly to the slurry under vigorous stirring. The support precursor, magnesium hydroxycarbonate (p.a.), was obtained from Riedel-de-Haën. A similar procedure was followed to prepare a catalyst (Fe/MgO) starting from MgO (Merck, p.a.).

Iron/alumina catalyst designated Fe/γ-Al_2O_3-Fe (the latter item refers to the species injected) was prepared by slow injection of a solution of $Fe(NO_3)_3 \cdot 9H_2O$ (0.179 mol $liter^{-1}$) at a rate of 2.0 μl s^{-1} into a suspension of γ-Al_2O_3 (Degussa-C) in initially 500 ml of water kept at pH 6.0 by controlled injection of a CO_2-free potassium hydroxide (Merck, p.a.) solution (3.56 mol $liter^{-1}$). The added amounts of $Fe(NO_3)_3 \cdot 9H_2O$ and γ-Al_2O_3 were 89 and 88 mmol, respectively.

Iron/alumina catalyst designated Fe/γ-Al_2O_3-OH was prepared by injection of CO_2-free potassium hydroxide (2.0 μl s^{-1}) into a solution of $Fe(NO_3)_3 \cdot 9H_2O$ and suspended γ-Al_2O_3, starting from a pH of 1.5. The amounts of chemicals used and the concentrations chosen were identical to those mentioned above.

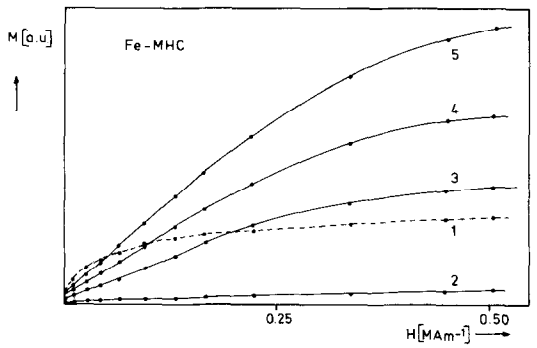

FIG. 1. M versus H curves for a 20 wt% Fe-MHC catalyst (referred to dry reduced sample) at successive stages of reduction with 10 vol% H_2/Ar. The succession is indicated by the numbers: (1) after reduction during 50 ks at 585 K (coded 50-585), (2) (60-645), (3) (30-750), (4) (20-785), and (5) (60-885).

A physical mixture of α-FeOOH and γ-Al_2O_3 (Degussa-C) was prepared in a weight ratio 1 : 4 (α-FeOOH/γ-Al_2O_3-Phys). α-FeOOH was precipitated by slow injection of $Fe(NO_3)_3 \cdot 9H_2O$ in the absence of a support material as described above. The α-Fe_2O_3 (p.a.) used in this study was supplied by Merck.

After filtration and subsequent washing with boiled demineralized water catalysts were dried at 323 K under vacuum during 16 ks, followed by drying for 60 ks at 368 K. After grinding, the catalysts were pressed at 75 MPa, the obtained pellets were crushed, and a sieve fraction of 0.5–0.7 mm was selected.

RESULTS

Iron/magnesia catalysts. Figure 1 presents curves of magnetization (M) versus magnetic field strength (H) for a 20 wt% Fe-MHC catalyst measured at successive stages of reduction in H_2/Ar. The magnetization was measured at ambient temperature. It should be emphasized that some hysteresis effects were apparent and that at the applied magnetic field strength saturation of the magnetization was not attained. It is obvious that the formation of a ferro- or ferrimagnetic phase is succeeded by the formation of a non-ferro/ferri-magnetic phase, while ultimately again a ferro/ferrimagnetic phase is formed. These observations are indicative of the successive formation of Fe_3O_4 or $MgFe_2O_4$ (both ferrimagnetic), FeO (paramagnetic or weak ferromagnetic) and α-Fe (ferromagnetic). The presence of α-Fe after reduction at 750 K and subsequent passivation was also established from X-ray diffraction patterns. From the diffuse spinel reflections observed after reduction up to 585 K we were unable to differentiate between the presence of $MgFe_2O_4$, Fe_3O_4, or a mixture of these compounds. Effluent gas analysis during the reduction demonstrated that on decomposition of the support precursor carbon dioxide evolves in addition to water. The carbon dioxide was partially reduced according to the reverse water-gas shift reaction, while finally also methanation activity was observed.

To exclude the possibility that the stabilization of a non-ferro/ferri-magnetic iron species is brought about by the composition of the gas phase during the reduction, an identical experiment was performed with a catalyst based on a MgO support instead of magnesium hydroxycarbonate, ensuring a well-defined gas phase during the reduction. The magnetization versus magnetic field strength curves shown in Fig. 2 for a 20 wt% Fe/MgO sample allow an analysis similar to that for the MHC based catalysts. Apart from the observation of $Mg(OH)_2$ lattice periodicities also d-spacings of 0.784,

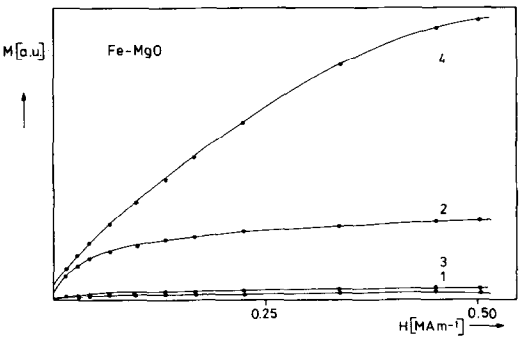

FIG. 2. M versus H curves for a 20 wt% Fe/MgO catalyst at successive stages of reduction with 10 vol% H_2/Ar. (1) Fresh sample, (2) after reduction during 12 ks at 573 K (12-573), (3) (4-663), and (4) (60-885).

0.399, 0.263, and 0.236 nm were calculated from the X-ray patterns. Assuming the Feitknecht compound to be of the 3R polytype (*19*) the above reflections were indexed as (003), (006), (009), and (105). The latter reflections were much more pronounced than those observed with the MHC-based catalyst of an identical metal loading.

Our MHC catalysts of low metal loading (3 wt% Fe) did not display the superparamagnetic behavior expected of very small iron particles, as was reported by Boudart *et al.* (*20*). After application of an identical reduction schedule no satisfactory superposition of magnetization versus magnetic field strength/temperature curves (indicative of superparamagnetic behavior) obtained at 298, 373, and 473 K was observed. Moreover, on subsequent evacuation of the sample, mass spectrometric analysis still revealed extensive evolution of carbon dioxide, giving rise to the partial reoxidation of the metallic phase.

Iron/alumina catalysts. In this section the reduction behavior of iron/alumina catalysts will be reported. To indicate the rationale underlying the experiments performed, a short introduction will be given. Apart from the thermodynamic driving force, the reduction process is considerably influenced by (i) the surface concentration of dislocations and point defects of the phase to be reduced, (ii) a chromatographic effect caused by the introduction of a highly porous support material, (iii) an intimate contact between the metal(oxide) phase and an oxide support, and (iv) the incorporation of ions originating from the support during coprecipitation. Although the individual contributions of the above effects to the observed reduction behavior are beyond experimental observation, we performed a series of experiments in which their respective contributions were varied to discriminate between the effects mentioned above as much as possible.

In Fig. 3a the temperature-programmed reduction profile of unsupported α-FeOOH is given. Calcination in a 10 vol% O_2/He

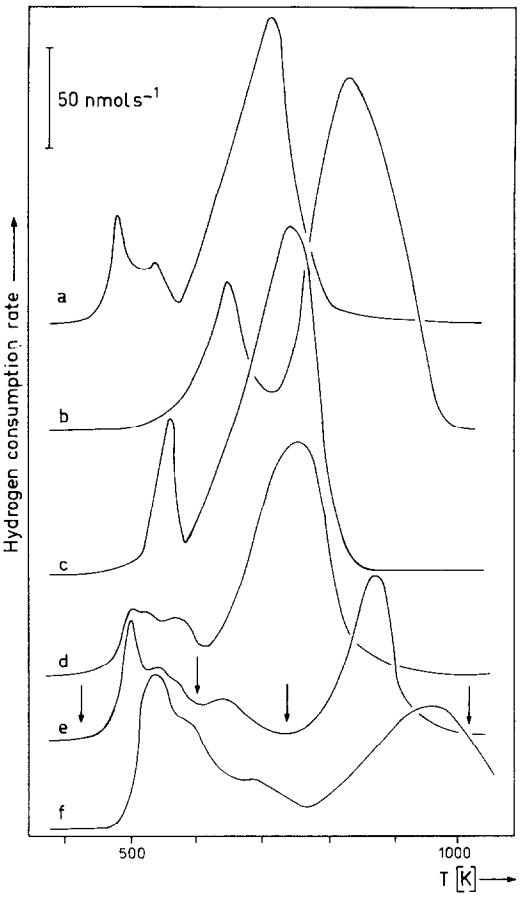

FIG. 3. TPR profiles measured in 10 vol% H_2/Ar at a flow rate of 0.8 ml s^{-1}. Heating rate 0.08 K s^{-1}. The amount of iron present in the samples was 0.25 mmol in all analyses shown. (a) α-FeOOH, (b) α-FeOOH calcined at 760 K during 100 ks, (c) α-Fe_2O_3, (d) α-FeOOH/γ-Al_2O_3-Phys, (e) Fe/γ-Al_2O_3-Fe, and (f) Fe/γ-Al_2O_3-OH. The arrows in indicate the temperatures at which the sample was quenched prior to subsequent characterization with X-ray analysis (see Fig. 7).

flow at 760 K for 100 ks preceding TPR causes the reduction pattern to be drastically modified (Fig. 3b). The three-peak pattern observed for the fresh α-FeOOH has changed into a two-peak pattern, characteristic of pure α-Fe_2O_3 as indicated in Fig. 3c. Physically mixing with γ-Al_2O_3 turns out to have a small effect on the reduction behavior of α-FeOOH, as demonstrated in Fig. 3d. The profiles for the Fe/γ-Al_2O_3-Fe and Fe/γ-Al_2O_3-OH catalysts are shown in Figs. 3e and f, respectively. X-

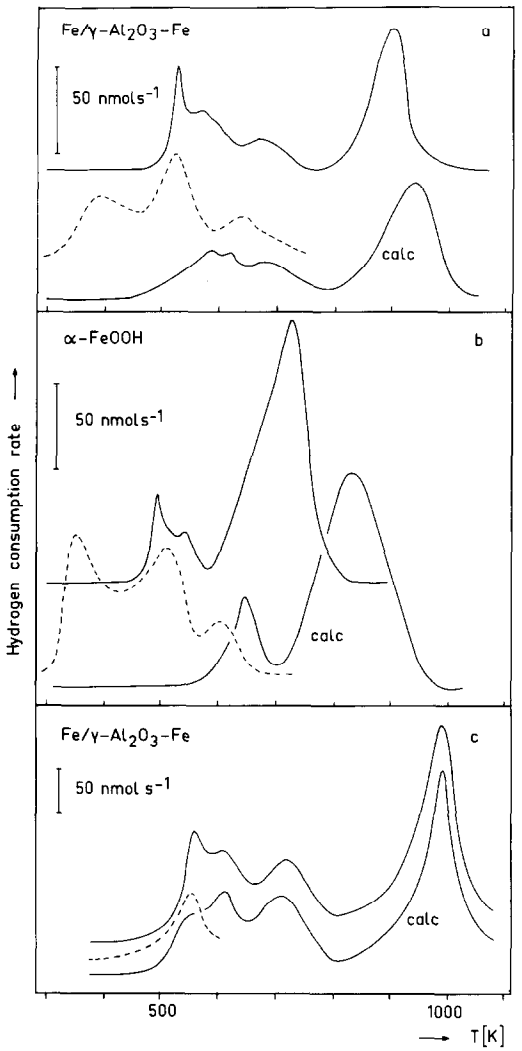

FIG. 4. TPR (—) and dehydration (----) profiles for Fe/γ-Al_2O_3-Fe and α-FeOOH (heating rate 0.08 K s^{-1}). The samples designated "calc" were calcined at 740 K prior to the reduction experiment. The amount of water evolved during the dehydration has not been determined quantitatively. In (c) TPR and dehydration profiles of the Fe/γ-Al_2O_3-Fe catalyst are collected (measured after prolonged drying) illustrating the effect of calcination at 585 K. For an optimal resolution of this pattern a heating rate of 0.16 K s^{-1} was applied.

Ray diffractograms demonstrated the presence of α-FeOOH in the samples α-FeOOH, α-FeOOH/γ-Al_2O_3-Phys, Fe/γ-Al_2O_3-Fe, and Fe/γ-Al_2O_3-OH prior to calcination or reduction.

In Fig. 4 the TPR profiles are given for the Fe/γ-Al_2O_3-Fe catalyst and for the α-FeOOH sample, both with and without previous calcination up to 740 K. Also the dehydration patterns are indicated, which were measured in a 10 vol% O_2/He flow. The onset temperature of reduction of the uncalcined samples is found to coincide exactly with that of the onset of the dehydration process succeeding the desorption of physically adsorbed water. Whereas a previous calcination shifts the onset temperature of reduction for the unsupported α-FeOOH to a significantly higher value, the onset for the supported catalyst has shifted to a lower temperature after calcination. The dehydration during temperature-programmed reduction of Fe/γ-Al_2O_3-Fe apparently gives rise to the formation of a highly defective α-Fe_2O_3, which is subject to simultaneous reduction. The unsupported α-FeOOH recrystallizes drastically during the calcination procedure, as was evidenced by the BET area which was reduced from 403 to 48 $m^2 g^{-1}$. The recrystallization affects also the surface concentration of defects resulting in a retarded onset of subsequent reduction. The first reduction peak which is rather sensitive to the calcination procedure applied thus turns out to be determined by the chemical nature of the iron phase (α-FeOOH or (sintered) α-Fe_2O_3). The reduction step starting at a temperature of about 570 K in the TPR of α-FeOOH has to be associated with the reduction from Fe_3O_4 to α-Fe which corresponds to about 86% of the total hydrogen consumption (the theoretical hydrogen consumption for this reaction amounts to 89%).

Let us now turn to the TPR profile for Fe/γ-Al_2O_3-Fe (Fig. 3e). A four-peak pattern is observed supporting our hypothesis that an intimate contact of the iron(oxide) phase with the support is accompanied by the presence of an FeO intermediate. In that case an extra peak in the TPR pattern would be expected, while also the reduction to α-Fe would be retarded. Comparison with the reduction profiles of α-

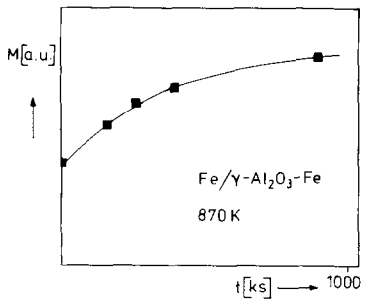

FIG. 5. Magnetization versus duration of reduction curve for a sample containing 1.0 mmol of Fe after temperature-programmed reduction up to 1010 K. Reduction was performed at 870 K in 10 vol% H_2/Ar at a flow rate of 0.8 ml s^{-1}.

FeOOH, on the other hand, suggests that we are dealing with a catalyst where part of the iron has precipitated as unsupported α-FeOOH. The increase of the rate of hydrogen consumption observed at 570 K with the Fe/γ-Al_2O_3-Fe catalyst could be tentatively ascribed to the reduction of Fe_3O_4 (originating from unsupported α-FeOOH) to α-Fe. It should be noted that especially the onset temperature of reduction contains information concerning the reduction process involved, whereas the temperature of maximum reduction rate depends on the amount of catalyst to be reduced. The drop in the hydrogen consumption during TPR at a temperature above 900 K suggests that the reduction process is completed within the time scale of the TPR experiment. Monitoring the magnetization at 0.52 MA m^{-1} as a function of time (Fig. 5) of a sample (containing 1.0 mmol of Fe) after temperature-programmed reduction up to 1010 K reveals that the reduction to α-Fe at 870 K is an extremely slow process. The magnetization was measured at ambient temperature after quenching the sample in the 10 vol% hydrogen/argon mixture. Figure 6 illustrates the influence of the quantity of iron used in the temperature-programmed reduction experiments. The hydrogen consumption measured for different reactor loadings is normalized to that for the sample containing 0.25 mmol of Fe. Evidently, the removal of water vapor determines the rate of the reduction to α-Fe. To collect further information on this catalyst we recorded X-ray diffraction patterns (Fig. 7) of the sample after quenching from the temperatures indicated by arrows in Fig. 3e, followed by careful static passivation. It should be pointed out that owing to a possibly extensive reoxidation the X-ray results should be interpreted with caution. After a rapid reduction to Fe_3O_4 the presence of FeO (d = 0.215 nm) is unambiguously demonstrated by the X-ray pattern obtained. The (200) reflection of FeO is no longer masked by broadened reflections originating from the support as was the case with MgO. The presence of α-Fe after quenching from 735 K was not established. Finally, it should be noted that

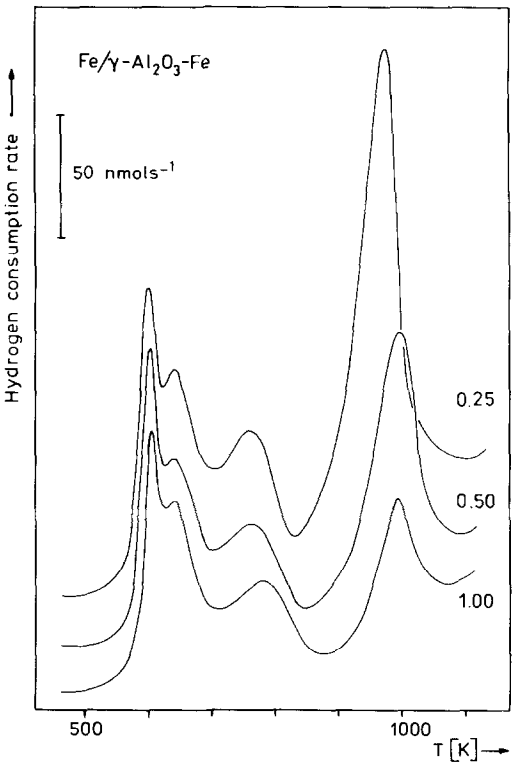

FIG. 6. TPR profiles for the Fe/γ-Al_2O_3-Fe catalyst at different reactor loadings. The amounts of Fe used for analysis (in mmol) are indicated. The hydrogen consumption detected is normalized to that of the sample containing 0.25 mmol of Fe. The applied heating rate was 0.16 K s^{-1}.

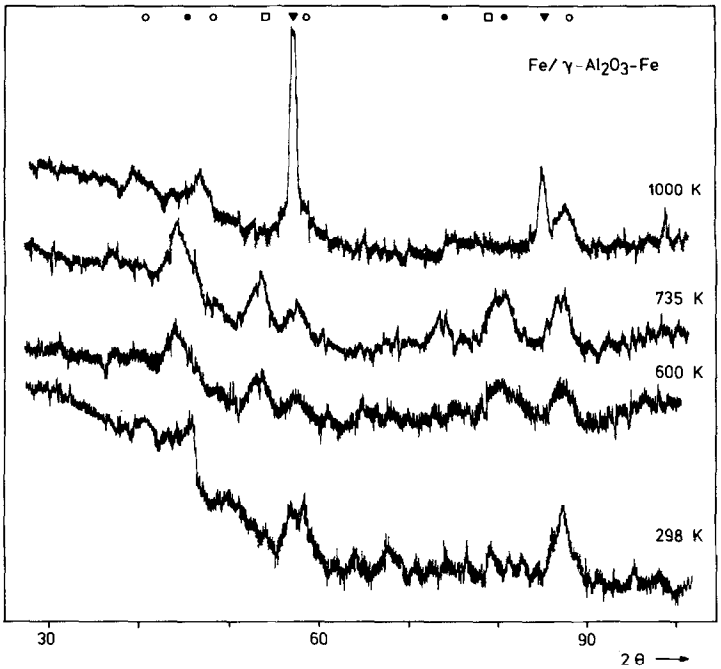

FIG. 7. X-Ray profiles for the Fe/γ-Al_2O_3-Fe catalyst recorded after quenching from (a) 600 K, (b) 735 K, and (c) 1000 K. The reflections originating from γ-Al_2O_3 (open circles), Fe_3O_4 (full circles), FeO (squares), and α-Fe (triangles) are indicated.

the TPR profile of the Fe/γ-Al_2O_3-OH sample shows an onset temperature of reduction (475 K) which is significantly higher than those observed with the samples discussed above.

X-Ray analysis and the measurement of M versus H curves at ambient temperature at regular intervals have the disadvantage that transient processes are possibly beyond experimental observation as a consequence of the selected frequency of analysis. Moreover, information concerning the sequence of the reduction stages can be lost, because also a quenching or passivation procedure has to precede the analysis. Therefore, we monitored *in situ* the magnetization at 0.52 MA m^{-1} during the temperature-programmed reduction. Actually, we perform thermomagnetic analysis on a chemically changing sample. To determine whether changes in the overall magnetization with increasing temperature are due to the proceeding of the reduction reaction or are merely due to the temperature dependence of the magnetization of a sample of a fixed composition, the temperature was incidentally temporarily lowered at the same rate. Changes in the magnetization at a given temperature contain information on the reduction process involved.

In Fig. 8 magnetization versus temperature curves during temperature-programmed reduction (MT-TPR) are given for the samples studied already with TPR. Reduction was performed in a 10 vol% hydrogen/argon mixture, while the heating rate was similar to that during TPR.

Thermomagnetic curves, recorded at declining temperature, immediately measured after reversal of the temperature program at 770 K, display (except for the samples α-FeOOH, α-Fe_2O_3, and α-FeOOH/γ-Al_2O_3-Phys) a decreased magnetization in the temperature region from about 650 to 770 K (as compared with the magnetization measured at increasing temperature). This is in-

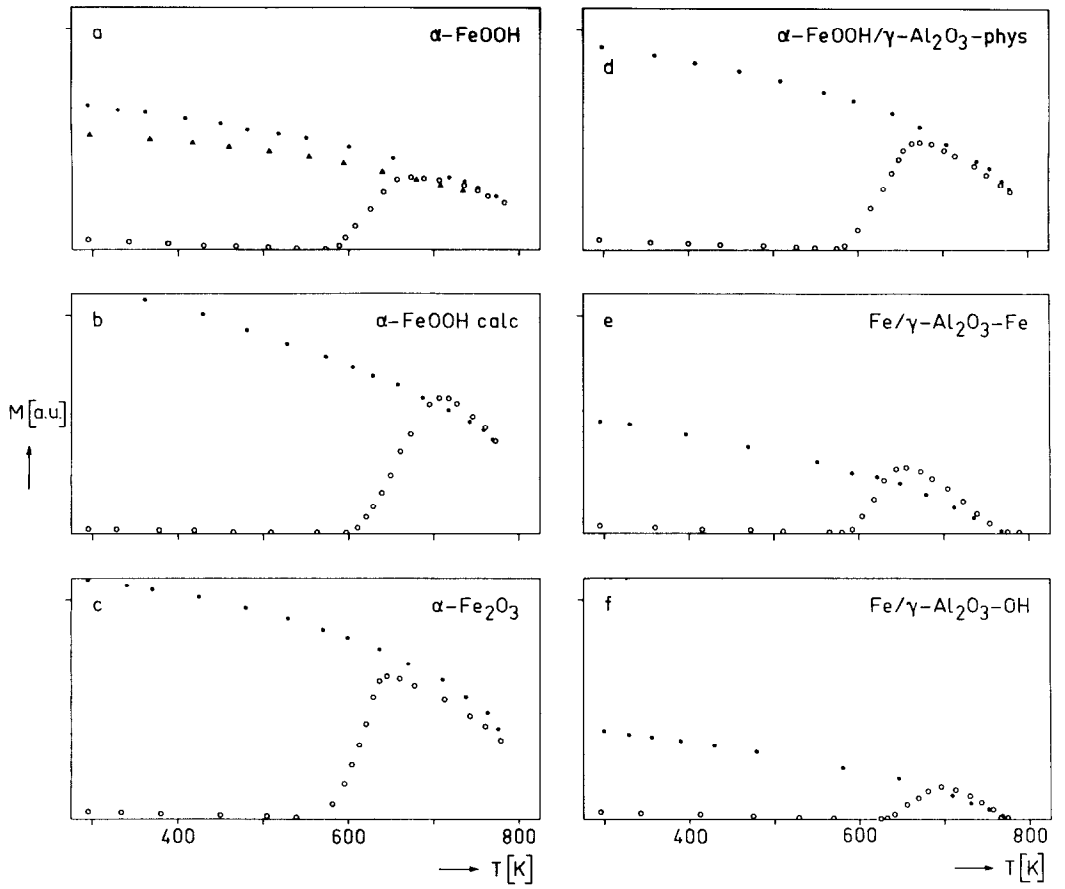

FIG. 8. (a–f) MT-TPR curves measured during reduction with 10 vol% H_2/Ar at a flow rate of 0.8 ml s^{-1}. The heating rate was 0.08 K s^{-1}. The part of the curve measured at rising temperature is indicated by open circles, while measurements at declining temperature are represented by full circles. In (a) measurements after the reversal of the temperature program at 740 K are indicated by triangles. The magnetic field strength applied was 0.52 MA m^{-1}.

dicative of the proceeding of the reduction process. In the case of unsupported α-FeOOH reversal of the temperature program at 740 K results also in a small decrease of the magnetization (as compared with the magnetization measured at increasing temperature). The presence of a ferro/ferrimagnetic phase with a Curie temperature of 760 ± 10 K is suggested from the MT-TPR curves (Figs. 8e and f). The onset temperature of reduction determined from these experiments is about 130 K higher than those observed during TPR. The dehydration treatment or the addition of γ-Al_2O_3 did not alter the onset temperature. In the case of Fe/γ-Al_2O_3-OH the reduction was retarded considerably in accordance with the TPR experiment. At first sight the MT-TPR and TPR results seem contradictory. Whereas the MT-TPR of the unsupported α-FeOOH shows a continuous decrease of the magnetization at rising temperature and does not display the increase of the magnetization due to the reduction to the ferromagnetic α-Fe, the TPR pattern suggests that the formation of α-Fe starts from 570 K. Holding the sample at 770 K results eventually in a gradual increase of the magnetization. Within the time scale of the MT-TPR experiment, however, the ex-

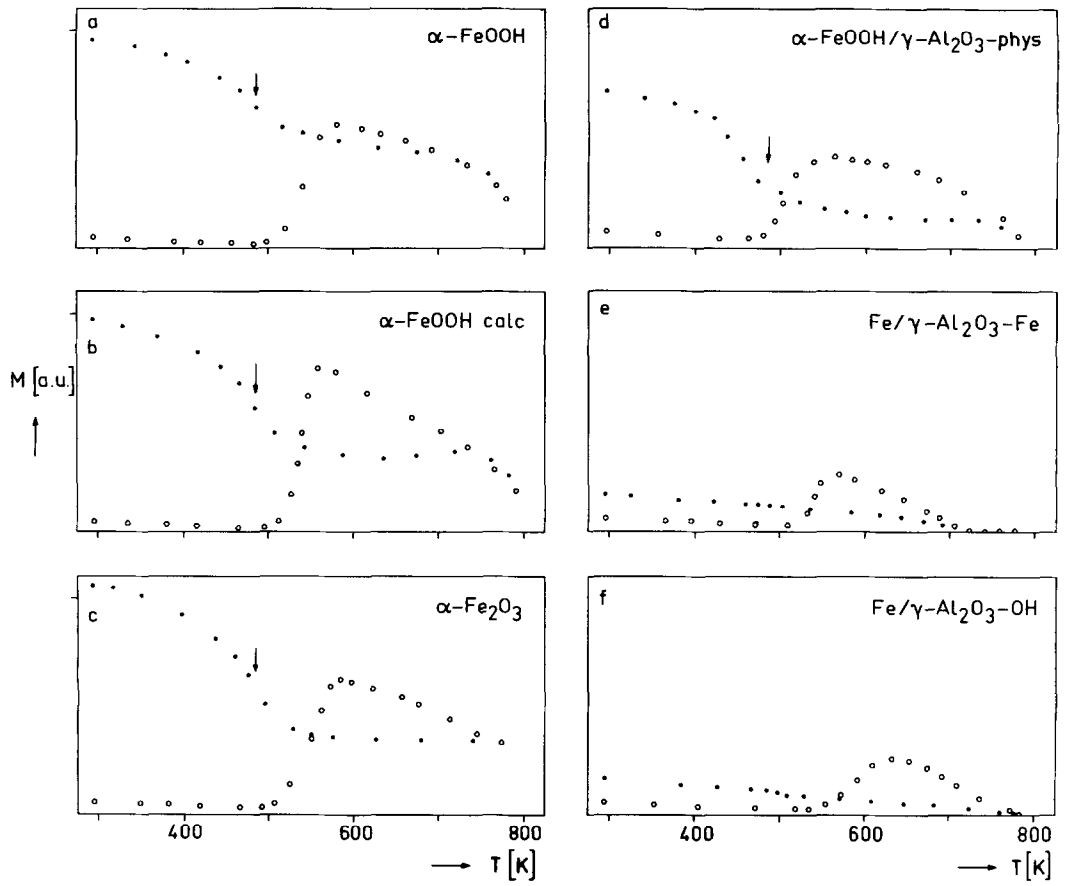

FIG. 9. (a–f) MT-TPR curves measured during reduction with 5 vol% CO/He at a flow rate of 0.8 ml s^{-1} (heating rate 0.08 K s^{-1}). Measurements made at rising and declining temperature are represented by open and full circles, respectively. The Curie temperature of θ-Fe_3C (483 K) is indicated by an arrow.

tent of the formation of ferromagnetic α-Fe is small.

Since the difference of the magnetization change at a given temperature observed with the supported catalysts does not differ considerably from that of the unsupported α-FeOOH, the MT-TPR technique (using hydrogen as reductant) does not supply a decisive experimental criterion for the presence of an iron species which has no marked interaction with the support.

As the onset temperature for the reduction with carbon monoxide is reported to be lower than that for reduction with hydrogen (*21*), we also collected MT-TPR curves with CO as reductant. In this case both the thermodynamic driving force and the kinetics of the reduction reaction are altered. This may afford the opportunity to vary the lifetime of the FeO intermediate sufficiently to allow testing of our hypothesis. The MT-TPR curves measured during reduction in a 5 vol% CO/He mixture are given in Fig. 9. A non-ferro/ferri-magnetic phase turns out to be exclusively stabilized in the samples Fe/γ-Al_2O_3-Fe and Fe/γ-Al_2O_3-OH. The formation of a carbidic phase preceding the reduction beyond FeO was contradicted both by the CO consumption and CO_2 production ratio (1.0) as well as by thermomagnetic analysis measured at declining temperature. The MT-TPR for unsupported

α-FeOOH, on the other hand, does not exhibit the exclusive stabilization of a nonferro/ferri-magnetic phase, while thermomagnetic analysis at declining temperature reveals the presence of θ-Fe_3C. Hence, we have a useful tool to assess whether part of the precipitated iron is present as unsupported α-FeOOH. Both the Fe/γ-Al_2O_3 catalysts are shown to have a considerable interaction with the support.

DISCUSSION

Iron/magnesia catalysts. The magnetization versus magnetic field strength curves for the 20 wt% Fe-MHC catalyst indicate that the reduction process from FeO to α-Fe is an extremely slow process. The FeO phase, stabilized by the formation of a solid solution with MgO, was evidenced by Boudart *et al.* (*17*) by analyzing the Fe^{2+} quadrupole splitting in the Mössbauer spectrum, which indicated that the Fe^{2+} is not homogeneously distributed in MgO, but tends to form Fe^{2+} clusters of an iron concentration nearly independent of the metal loading. However, their observation that the fraction of metallic iron after reduction is independent of the metal loading seems rather fortuitous in the light of our observations on the reduction behavior. The applied reduction procedure will strongly determine the degree of reduction ultimately attained.

The *d*-spacings reported by the authors mentioned above (0.797, 0.400, and 0.264 nm), are indicative of the formation of a Feitknecht compound during precipitation and subsequent ageing. The observation that a Feitknecht compound is also formed in the case of precipitation on MgO as well as in the case of coprecipitation (*17*) suggests that the Mg^{2+} concentration during precipitation determines whether a bulk sjögrenite/pyroaurite phase [$Mg_xFe_y(OH^-)_{2x+3y-2z}(CO_3^{2-})_z \cdot nH_2O$, where CO_3^{2-} may be substituted by other anions] is formed. Precipitation at low Mg^{2+} concentrations may be restricted to an exchange of Mg^{2+} ions by Fe^{3+} ions as described by Topsøe *et al.* (*22*). The stoichiometry of the Feitknecht compound formed (generally x/y ratios between 1.5 and 4.0 are observed (*19*)) will possibly depend on the concentration ratio of Mg^{2+} and Fe^{3+} ions during precipitation. The realized Mg^{2+} concentration is related to the reactivity of the support (-precursor), which turns out to differ considerably for various support materials. Analysis of electron micrographs (not shown) revealed that even after ageing for 60 ks at 343 K the structure of the original MHC was still preserved, whereas after only 2 ks the structure of the original MgO was completely absent and hexagonal $Mg(OH)_2$ platelets were formed. As expected from this observation, particularly in the case of the MgO-based catalyst, the presence of a well-ordered Feitknecht compound was confirmed by X-ray patterns. The inert nature of the MHC material used in our experiments probably explains the discrepancy with the earlier observations by Boudart *et al.* (*17*). The low magnesium concentration brings about the deposition of an iron-rich phase leading to large particles on reduction.

The formation of a Feitknecht compound also accounts for the observation that the Fe^{2+} concentration is enhanced as compared to a homogeneous distribution over the MgO phase. Iron and magnesium ions are mixed on an atomic scale which causes the reduction beyond Fe^{2+} to be strongly retarded.

In a study on MHC-based iron catalysts thermomagnetic analysis was applied to investigate the effects of thermal decomposition *in vacuo,* calcination in air or reduction (*23*). It was concluded that (i) the Curie temperature of α-Fe was lowered by about 190 K, (ii) after reduction at 700 K the presence of $MgFe_2O_4$ was still observed, whereas earlier Mössbauer experiments only revealed the presence of α-Fe and Fe^{2+} (*17*), and (iii) an FeO phase is formed originating from the reaction $MgFe_2O_4$ + Fe $\rightarrow$ MgO + 3 FeO. In the opinion of the present authors a drop in the Curie temper-

ature of α-Fe of about 190 K is rather large for particles of a size which still allows detection by means of X-ray diffraction. For comparison the lowering of the Curie temperature of nickel particles (3.0–8.5 nm diameter) also stabilized by an oxidic support, amounts to about 50 K (*24*), while in a review Jacobs and Bean (*25*) concluded that only granular metal films of a thickness below 2.0 nm, deposited on various substrates, display minor changes in the Curie temperature. Although examples are known where Mössbauer spectroscopy failed to demonstrate directly the presence of poorly ordered Fe^{3+}, for instance, after passivation in air (*26*), it should be questioned whether the interpretation of the thermomagnetic curves, viz. the presence of Fe^{3+} (in magnesium ferrite), presented in the above-mentioned paper (*23*) is correct. Whereas the maximum reduction temperature applied in the latter investigation was 700 K, the thermomagnetic analysis was performed up to 870 K. The increase of the magnetization observed around a temperature of 700 K (assumed to be indicative of the presence of $MgFe_2O_4$) may be ascribed to the thermally induced disproportionation of the non-ferro/ferri-magnetic FeO to Fe_3O_4 and α-Fe. The absence of α-Fe deduced from the thermomagnetic analysis, which is probably due to reoxidation of the α-Fe by carbon dioxide and water formed on the decomposition of the support precursor, will be discussed later in this paper. Moreover, it is questionable whether a straightforward characterization of the $MgFe_2O_4$ phase on the basis of its Curie temperature is possible, considering the broad range of Curie temperatures reported and its delicate dependence on the distribution of Mg^{2+} ions over octahedral and tetrahedral sites in the spinel structure (*27–29*). Our magnetization versus magnetic field strength curves collected at ambient temperature demonstrate clearly that the FeO phase can be isolated almost exclusively. This indicates that FeO is an intermediate rather than the product from the reaction between $MgFe_2O_4$ and α-Fe, which must be present in balanced amounts to explain the complete disappearance of the ferro/ferrimagnetism.

Iron/alumina catalysts. A first remark should be made about the catalyst preparation method used. Dousma and de Bruyn (*30, 31*) demonstrated that hydrolysis and subsequent olation and oxolation of Fe^{3+} salts leads to the formation of small colloidal particles of FeOOH of a remarkable stability. It is evident that precipitation from an acid $Fe(NO_3)_3 \cdot 9H_2O$ solution (pH approximately 1.5) by injection of a base results in the gradual formation of these colloidal particles which are supposed to have little interaction with the support. Therefore, we injected the iron nitrate solution into a suspension of the support, kept at pH 6.0, thus preventing also the partial dissolution of the Al_2O_3 support (*32*). The Fe/γ-Al_2O_3-Fe catalyst turns out to be in intimate contact with the support as proven by the carbon monoxide MT-TPR experiment. The shift to lower onset temperatures of reduction after calcination is another indication that the iron phase is well-dispersed on the support, preventing the sintering observed with the unsupported α-FeOOH.

Also the hydrated iron oxide species in the Fe/γ-Al_2O_3-OH catalyst appears to have a considerable interaction with the support. The retarded onset of reduction indicates that aluminum ions, liberated from the support at pH values below 4, are incorporated in the iron oxyhydroxide structure.

Monitoring of the magnetization during temperature-programmed reduction by carbon monoxide has been demonstrated to be an elegant method to establish whether the precipitate has been deposited onto the support. The method is considered to be of particular importance when electron microscopic analysis, which is one of the most powerful techniques to establish directly the nature of a catalyst, fails to reveal information. The well-crystallized γ-Al_2O_3 support, for instance, brings about extensive diffraction contrast in transmission electron

micrographs. The contrast arising from the iron phase, which causes relatively more incoherent elastic electron scattering than the surrounding support ("Z"-contrast), is completely dominated by the diffraction contrast from the support. Only laborious application of dark-field imaging techniques using identified diffracted beams will provide information. Moreover, the application of electron microscopy asks for additional characterization as heterogeneity of the sample may be overlooked.

From the work presented in this paper it may be concluded that performing TPR experiments without the use of an additional *in situ* characterization technique is of limited use for the characterization of iron catalysts. However, a drawback of the combination of TPR and magnetic methods has to be mentioned, too. Due to the dynamic character of the techniques employed, part of the reduction process can be beyond experimental observation, as evidenced by recording the magnetization as a function of time during reduction at 870 K (Fig. 5). As the temperature region can only be extended to above 1073 K at the risk of the involvement of solid-state reactions between the active phase and the support, we have to derive information from the nature and kinetic stability of the (partially) reduced phases. The concept that the lifetime of the intermediate metastable FeO phase is associated with an interaction with the support appeared to be a useful one in the characterization of iron catalysts. Characterization of carbon- and silica-based catalysts in the way outlined above is in progress, and will be reported in due course.

In the Results section we associated the non-ferro/ferri-magnetic phase with FeO. The present authors do not claim to have identified a well-defined FeO phase. Already in the past (*33, 34*) it has been reported that FeO forms a solid solution with Fe_3O_4 as well as with α-Fe. On decomposition of FeO, prepared by quenching from temperatures above 843 K, it was established with magnetic measurements that free metallic iron exhibiting ferromagnetic behavior was not observed at temperatures below 723 K, while the formation of magnetite started from 560 K onward. Moreover, on decomposition of FeO, reflections due to Fe appeared much later than those due to Fe_3O_4. Thus, the disappearance of ferro/ferrimagnetism points to an FeO phase, which still can contain amounts of Fe_3O_4 or Fe. This reasonably accounts for the apparent discrepancy between the onset temperatures of reduction to α-Fe deduced from TPR and MT-TPR experiments. At the beginning of the reduction to metallic iron a solid solution of Fe in FeO is formed which does not exhibit ferromagnetism. The absence of metallic iron, as observed by Derouane (*23*), can also be interpreted in terms of a nonferromagnetic solid solution of Fe in FeO.

The difference between the onset temperatures of reduction to magnetite (about 130 K higher in the MT-TPR experiment than with TPR) can be explained by realizing that during the reduction of Fe_2O_3 to Fe_3O_4 initially a poorly ordered Fe_3O_4 is formed which does not exhibit ferrimagnetism. Although it has been reported that Fe_3O_4 should form a solid solution with α-Fe_2O_3 (*35*), this concept has not found general acceptance. Furthermore, superparamagnetic Fe_3O_4 particles of a diameter less than 1.0 nm are beyond detection. The formation of these particles at the start of the reduction would also explain the observed differences between the onset temperatures of reduction. The possibility that these differences are completely due to variations in the experimental setup can be excluded. Both types of experiments were performed in a flow-through reactor, while the temperature was measured at the center of the catalyst bed. Radial and axial temperature gradients were completely negligible in view of the magnitude of the observed differences. Performing temperature-programmed reduction in the reactor used in the MT-TPR experiment, the onset of reduction to Fe_3O_4 was found to be unchanged, whereas the

onset of the reduction to α-Fe was retarded by 90 K, predominantly due to the larger amount of sample used. From Fig. 6 it emerges that MT-TPR or TPR experiments can only be mutually compared when the amount of water to be removed is equal. In the case of catalysts with a considerable metal loading, this demand is met when the amount of iron present in the sample is constant.

In the case of alumina-containing samples also the presence of $FeAl_2O_4$ can be expected (*2, 36, 37*), formed during the reduction process. This compound is paramagnetic at the temperatures at which the thermomagnetic analysis was performed, so our magnetic investigation does not contain any information about the involvement of $FeAl_2O_4$. X-Ray patterns did not reveal its presence.

The observation of a reflection corresponding with a *d*-spacing of 0.215 nm, which unambiguously arises from FeO, was also observed at temperatures from 633 K onward by Gaballah *et al.* (*38*) performing *in situ* diffraction techniques during the reduction of Fe_3O_4 by hydrogen. Romanov (*39*) revealed the presence of wustite during the reduction of Fe_2O_3, using Mössbauer spectroscopy.

Finally, we wish to comment on the relevance of the establishment of the presence of an FeO phase prior to reduction to α-Fe. The distinct stabilization of the FeO phase suggests that apart from changes in the kinetics of the reduction also the thermodynamics are influenced by the interaction with the support. When the stabilization by the support lowers the Gibbs free energy function of FeO with respect to the sum of the Gibbs free energy functions of the equivalent amounts of Fe_3O_4 and α-Fe, the thermodynamic driving force for the reduction beyond stabilized FeO has apparently decreased. Progress of the reduction beyond FeO at a given ratio of partial pressures of hydrogen and water calls for a higher reduction temperature.

CONCLUSIONS

Our conclusions are as follows:

(i) Preparation of iron/magnesia catalysts by injection of iron nitrate into a suspension of magnesium hydroxycarbonate or magnesium oxide results in the formation of Feitknecht compounds. During reduction of the samples by hydrogen complete disappearance of ferro/ferrimagnetic behavior was observed, indicative of the presence of an intermediate FeO phase stabilized by the support.

(ii) The concept that the lifetime of an FeO phase can be considered as an indication that the iron phase has considerable interaction with the support is shown to be useful in the characterization of iron/alumina catalysts. Monitoring of the magnetization during temperature-programmed reduction with carbon monoxide as reductant excluded the possibility that the precipitated iron is partially present as unsupported α-FeOOH in the Fe/Al_2O_3 catalysts investigated.

(iii) Iron carbides were not formed preceding the reduction beyond FeO during the reduction of the Fe/γ-Al_2O_3 catalysts with carbon monoxide.

ACKNOWLEDGMENTS

The authors are indebted to Mr. E. Boellaard and Mr. M. van der Meer for their contribution to the experimental work. The investigations were supported by the Netherlands Foundation for Chemical Research (SON) with financial aid from the Netherlands Organization for the Advancement of Pure Research (ZWO). Finally, the authors wish to express their appreciation to Mr. P. K. de Bokx for helpful discussions.

REFERENCES

1. Shimokawabe, M., Furuchi, R., and Ishii, T., *Thermochim. Acta* **28,** 287 (1979).
2. Brown, R., Cooper, M. E., and Whan, D. A., *Appl. Catal.* **3,** 177 (1982).
3. Sastri, M. V. C., Viswanath, R. P., and Viswanathan, B., *Int. J. Hydrogen Energy* **7,** 951 (1982).
4. Unmuth, E. E., Schwartz, L. H., and Butt, J. B., *J. Catal.* **61,** 39 (1980).
5. Hurst, N. W., Gentry, J., Jones, A., and McNicol, B. D., *Catal. Rev.-Sci. Eng.* **24**(2), 253 (1982).

6. Baranski, A., Lagan, M., Pattek, A., and Reizer, A., *React. Kinet. Catal. Lett.* **15,** 285 (1980).
7. Baranski, A., Lagan, M., Pattek, A., Reizer, A., Christiansen, L. J., and Topsøc, H., *in* "Studies in Surface Science and Catalysis" (B. Delmon, P. Grange, P. A. Jacobs, and G. Poncelet, Eds.), Vol. 3, p. 353. Elsevier, Amsterdam, 1979.
8. Spitzer, R. H., Manning, F. S., and Philbrook W. O., *Trans. Met. Soc. AIME* **236,** 725 (1966).
9. McKewan, W. M., *Trans. Met. Soc. AIME* **218,** 2 (1960).
10. Themelis, N. J., and Gauvin, W. H., *Trans. Met. Soc. AIME* **227,** 190 (1963).
11. Baranski, A., Lagan, M., Pattek, A., and Reizer, A., *Appl. Catal.* **3,** 201 (1982).
12. Baranski, A., Lagan, M., Pattek, A., and Reizer, A., *Appl. Catal.* **3,** 207 (1982).
13. Pattek-Janczyk, A., and Hrynkiewicz, A. Z., *Appl. Catal.* **6,** 27 (1983).
14. Amenomiya, Y., and Pleizier, G., *J. Catal.* **28,** 442 (1973).
15. Garten, R. L., and Ollis, D. F., *J. Catal.* **35,** 232 (1974).
16. Hobson, M. C., and Campbell, A. D., *J. Catal.* **8,** 294 (1967).
17. Boudart, M., Delbouille, A., Dumesic, J. A., Khammouma, S., and Topsøe, H., *J. Catal.* **37,** 486 (1975).
18. Kock, A. J. H. M., de Bokx, P. K., Boellaard, E., and Geus, J. W., *J. Catal.*, in press.
19. Puxley, D. C., Kitchener, I. J., Komodromos, C., and Parkyns, N. D., *in* "Studies in Surface Science and Catalysis" (G. Poncelet, P. Grange, and P. A. Jacobs, Eds.), Vol. 16, p. 237. Elsevier, Amsterdam, 1983.
20. Boudart, M., Dumesic, J. A., and Topsøe, H., *Proc. Natl. Acad. Sci. USA* **74,** 806 (1977).
21. Richard, M. A., Soled, S. L., Fiato, R. A., and DeRites, B. A., *Mater. Res. Bull.* **18,** 829 (1983).
22. Topsøe, H., Dumesic, J. A., Derouane, E. G., Clausen, B. S., Mørup, S., Villadsen, J., and Topsøe, N., *in* "Studies in Surface Science and Catalysis" (B. Delmon, P. Grange, P. A. Jacobs, and G. Poncelet, Eds.), Vol. 3, p. 365. Elsevier, Amsterdam, 1979.
23. Derouane, G., *in* "Reactivity of Solids" (J. Wood, O. Lindqvist, C. Helgesson, and N. Vannerberg, Eds.), p. 559. Plenum, New York, 1977.
24. Abeledo C., and Selwood, P. W., *J. Appl. Phys.* **32,** Suppl. 318S (1961).
25. Jacobs, I. S., and Bean, C. P., *in* "Magnetism: A Treatise on Modern Theory and Materials" (G. T. Rado and H. Suhl, Eds.), Vol. 3, p. 271. Academic Press, New York, 1963.
26. Topsøe, H., Dumesic, J. A., and Boudart, M., *J. Catal.* **28,** 477 (1973).
27. Kriessman, C. J., and Harrison, S. E., *Phys. Rev.* **103,** 857 (1956).
28. Epstein, D. J., and Frackiewicz, B., *J. Appl. Phys.* **29,** 376 (1958).
29. Landolt-Börnstein, *in* "Crystal and Solid State Physics" (K.-H. Hellwege and A. M. Hellwege, Eds.), Vol. III-4b, p. 217. Springer-Verlag, Berlin, 1970.
30. Dousma, J., and de Bruyn, P. L., *J. Colloid Interface Sci.* **56,** 527 (1976).
31. Dousma, J., and de Bruyn, P. L., *J. Colloid Interface Sci.* **64,** 154 (1978).
32. Perrichon, V., Charcosset, H., Barrault, J., and Forquy, C., *Appl. Catal.* **7,** 21 (1983).
33. Bénard, J., *Ann. Chim.* **11,** 12-5 (1939).
34. Colombo, U., Gazzarrini F., and Lanzavecchia, G., *Mater. Sci. Eng.* **2,** 125 (1967).
35. Huggett, J., and Chaudron, G., *C. R.* **184,** 199 (1927).
36. Tittle, K., *Proc. Aust. Inst. Min. Metall.* **243,** 57 (1972).
37. Smith, P. J., Taylor, D. W., Dowden, D. A., Kemball, C., and Taylor, D., *Appl. Catal.* **3,** 303 (1982).
38. Gaballah, I., Gleitzer, C., and Aubry, J., *in* "Reactivity of Solids" (J. Wood, O. Lindqvist, C. Helgesson, and N. Vannerberg, Eds.), p. 391. Plenum, New York, 1977.
39. Romanov, V. P., Checherskaya, L. F., and Tatsienko, P. A., *Phys. Status Solidi A* **15,** 721 (1973).